Available online at www.sciencedirect.com
SCIENCE DIRECT
Journal of Catalysis 238 (2006) 301–308
JOURNAL OF CATALYSIS
www.elsevier.com/locate/jcat

Reactions of hydroxymatairesinol over supported palladium catalysts

Heidi Markus [a], Päivi Mäki-Arvela [a], Narendra Kumar [a], Teemu Heikkilä [b], Vesa-Pekka Lehto [b], Rainer Sjöholm [c], Bjarne Holmbom [d], Tapio Salmi [a], Dmitry Yu. Murzin [a,*]

[a] *Laboratory of Industrial Chemistry, Process Chemistry Centre, Åbo Akademi University, Biskopsgatan 8, FIN-20500 Åbo/Turku, Finland*
[b] *Department of Physics, University of Turku, FIN-20014 Åbo/Turku, Finland*
[c] *Department of Organic Chemistry, Process Chemistry Centre, Åbo Akademi University, Biskopsgatan 8, FIN-20500 Åbo/Turku, Finland*
[d] *Laboratory of Wood and Paper Chemistry, Process Chemistry Centre, Åbo Akademi University, Porthansgatan 3, FIN-20500 Åbo/Turku, Finland*

Received 3 July 2005; revised 19 December 2005; accepted 19 December 2005

Available online 20 January 2006

Abstract

In this work, hydroxymatairesinol (extracted from Norway spruce knots) was hydrogenolyzed to matairesinol over palladium impregnated H-Beta-300, H-Beta-150, H-Beta-25, H-Beta-11, H-Y, H-Mordenite, H-MCM-41, H-ZSM-5, SiO_2, and Al_2O_3. H-Beta-25 without palladium was also investigated. The hydrogenolysis was performed in 2-propanol at 70 °C under hydrogen and nitrogen atmospheres in a stirred glass reactor. The catalysts were characterized by nitrogen physisorption, direct current plasma atomic emission spectrometry, X-ray powder diffraction, CO pulse chemisorption, transmission electron microscopy, and Fourier transform infrared spectroscopy (pyridine adsorption). Palladium on H-Beta with different acidities was tested; the results showed that the reaction rate was inversely proportional to the acidity. However, Brønsted acid sites are needed for the reaction, because palladium on SiO_2 and Al_2O_3 is not active. In addition to the acidity, a metal is needed; the H-Beta-25 support without palladium displays no activity.

Keywords: Lignans; Hydroxymatairesinol; Matairesinol; Oxomatairesinol; Hydrogenolysis; Zeolites; Acidity

1. Introduction

Previous studies have suggested that lignans have a preventive effect against hormone-dependent cancers, such as breast, prostate, and colon cancers [1]. In addition to the anticarcinogenic effects, they also have antioxidative effects [2]. Lignans, a group of plant phenols consisting of two β–β-linked cinnamic acid residues [3], can be found in many different parts of plants, including the woody parts, roots, leaves, flowers, fruits, and seeds. Most plants contain small amounts of lignans as glycosidic conjugates associated with fiber components, complicating the isolation process [4]. Coniferous trees, in contrast, contain large amounts of lignans in unconjugated forms, which can be more easily isolated. Knots (i.e., the part of the branch embedded in the stem) of Norway spruce (*Picea abies*) contain large quantities of lignans (6–24 wt%), of which hydroxymatairesinol is the most abundant (65–85 wt% of the lignans) [5]. There are two diastereomers of hydroxymatairesinol, (7*R*,8*R*,8′*R*)-(–)-7-allo-hydroxymatairesinol (HMR 1) and (7*S*,8*R*,8′*R*)-(–)-7-hydroxymatairesinol (HMR 2), of which the latter is the dominating isomer [6].

Matairesinol (MAT) can be found in small amounts in different plants, including flax and rye [7]. MAT can be produced through hydrogenolysis of HMR, which, as indicated above, can be extracted in larger amounts from Norway spruce knots. Hydrogenolysis of benzyl alcohol derivatives has been performed over carbon-supported palladium catalysts in ethanol [8]. Although hydroxyl is a poor leaving group, the reaction rate can be enhanced considerably by adding an acid, which produces a protonated alcohol, making water the leaving group [8,9]. Markus et al. [10] hydrogenolyzed HMR over Pd/C in 2-propanol and found that the carbon's acidity had a profound effect on the activity; the reaction rate increased with increasing acidity. However, carbon-supported metal catalysts can exhibit large batch-to-batch variations, due to, for exam-

* Corresponding author. Fax: +358 2 215 4479.
E-mail address: dmurzin@abo.fi (D.Yu. Murzin).

0021-9517/$ – see front matter
doi:10.1016/j.jcat.2005.12.022

ple, natural variations in the starting material [11]; moreover, the reproducibility of the catalyst preparation with respect to the surface groups may become difficult. Zeolites, crystalline aluminosilicates with varying structures and acidities during synthesis, have been used very successfully in hydrocarbon processing, but their use in fine chemical synthesis is still in a relatively early state of development [12,13].

Because in earlier work [10] we found that a more acidic carbon support was more active in hydrogenolysis than a less acidic carbon support, in the present work we investigated the possibility of using zeolites impregnated with palladium. An important advantage of zeolites is that they can be readily synthesized in a reproducible manner. In this work, a mixture of HMR isomers (HMR 1 and 2) extracted from Norway spruce was hydrogenolyzed to MAT over palladium-impregnated H-Beta-300, H-Beta-150, H-Beta-25, H-Beta-11, H-Y, H-Mordenite, H-MCM-41, H-ZSM-5, SiO_2, and Al_2O_3. H-Beta-25 without palladium was also investigated. The influence of the initial ratio of isomers to reduction temperature was studied as well.

Hydrogenolysis was performed in 2-propanol at 70 °C under hydrogen and nitrogen atmospheres in a stirred glass reactor. The reaction scheme is depicted in Fig. 1a, and the difference between the isomers is illustrated in Fig. 1b. The catalysts were characterized by nitrogen physisorption, direct current plasma atomic emission spectrometry (DCP), X-ray powder diffraction (XRPD), CO pulse chemisorption, transmission electron microscopy (TEM), and Fourier transform infrared spectroscopy (FTIR; pyridine adsorption).

2. Experimental

2.1. Synthesis of HMR

HMR was isolated from Norway spruce knots as follows. First, the knots were ground and extracted in an acetone–water mixture (90:1 vol/vol). Then the extract was concentrated in a rotary evaporator and purified by flash chromatography on silica (eluent dichloromethane:ethanol, 97.5:2.5 vol/vol) to yield a pure HMR solution, which was evaporated in the rotary evaporator. The material was 93% pure as determined by gas chromatography. The major impurity was the lignan conidendrin. The HMR 1/HMR 2 ratio was approximately 1:3.

2.2. Catalysts

Palladium (5 wt% nominal loading)-impregnated H-Beta-300, H-Beta-150, H-Beta-25, H-Beta-11, H-Y, H-Mordenite, H-ZSM-5, H-MCM-41, SiO_2, and Al_2O_3 were synthesized as follows. NH_4-Beta-300, NH_4-Beta-150, NH_4-Beta-25, NH_4-Mordenite-20, and NH_4-Y-12 zeolites (SiO_2/Al_2O_3 molar ratios of 300, 150, 25, 20, and 12, respectively) were supplied by Zeolyst International, SiO_2 was provided by Merck, and Al_2O_3 was obtained from UOP. The proton forms of the zeolites were obtained through calcination of the NH_4 form of the materials in a muffle oven at 500 °C for 4 h (at a heating rate of 5 °C/min). Na-Beta-11 zeolite (Si/Al weight ratio 11) was synthesized as described previously [14] with some modification. A solution was prepared by mixing colloidal silica (Ludox As 40, Aldrich) with distilled water. Another solution was prepared by dissolving sodium aluminate ($NaAlO_2$) in distilled water and adding tetraethylammonium hydroxide ($(C_2H_5)_4NOH$, Fluka). The two solutions were mixed together and stirred for a while. The gel thus formed was transferred into a Teflon cup, which was inserted into a 300-ml stainless steel autoclave (Parr Instruments). The synthesis was carried out at 150 °C for 96 h. After completion, the autoclave was quenched and the crystalline product was filtered, washed with distilled water, dried at 100 °C for 12 h, and calcined at 550 °C for 9 h in a muffle oven (at a heating rate of 5 °C/min). Na-ZSM-5 zeolite was synthesized in an autoclave at 150 °C for 48 h as described previously [15] with some modifications. The reagents used in the synthesis were fumed silica (SiO_2, Aldrich), sodium hydroxide (NaOH, Merck), aluminium hydroxide ($Al(OH)_3$, Aldrich), tetrapropylammonium bromide ($(C_3H_7)_4NBr$, Fluka), and distilled water. After synthesis was complete, the autoclave was quenched in cold water, and the synthesized materials were filtered and washed thoroughly with distilled water. Na-ZSM-5 samples were dried at 100 °C for 12 h, and templates were removed by calcination at 540 °C for 8 h (at a heating rate of 5 °C/min). Synthesis of Na-MCM-41 mesoporous molecular sieve was conducted in an autoclave as described previously [16] with some modifications. The synthesis was performed by preparing solutions A, B, and C. Solution A was prepared by mixing fumed silica (SiO_2, Aldrich) with distilled water under continuous stirring. Solution B was prepared by adding tetramethylammonium silicate ($(CH_3)_4NOH{\cdot}2SiO_2$, Aldrich) to sodium silicate (Na_4O_4Si, Merck) and stirring for 15 min. Solution C was prepared by dissolving tetradecyltrimethylammonium bromide ($C_{17}H_{38}BrN$, Aldrich) in distilled water. Solution B was slowly added to solution A and stirred for 20 min. Subsequently, solution C was introduced under vigorous stirring. A required amount of aluminium isopropoxide ($[(CH_3)_2CHO]_3Al$, Aldrich) was mixed, and the gel solution was stirred for 30 min. After the pH of the prepared gel was measured, the gel was placed in a Teflon cup, which was then inserted into an autoclave. The synthesis was performed at 100 °C in an oven for 24 h. After completion of the synthesis, the reactor was quenched, and the mesoporous material was filtered and washed thoroughly with distilled water. Na-MCM-41 was dried at 110 °C for 12 h and calcined at 550 °C for 10 h (at a heating rate of 5 °C/min). The sodium forms of Beta-11, ZSM-5, and MCM-41 were ion-exchanged with 1 M ammonium chloride (NH_4Cl) for 48 h and washed with distilled water to remove any chloride ions. After subsequent drying at 100 °C for 12 h, the proton forms were obtained by calcination of NH_4 forms at 500 °C for 4 h (at a heating rate of 5 °C/min). The support materials were impregnated with palladium by the vacuum evaporation impregnation method in a rotary evaporator, using aqueous solution of palladium nitrate as a precursor. The catalysts were dried at 110 °C for 12 h and calcined at 400 °C for 3 h (at a heating rate of 5 °C/min).

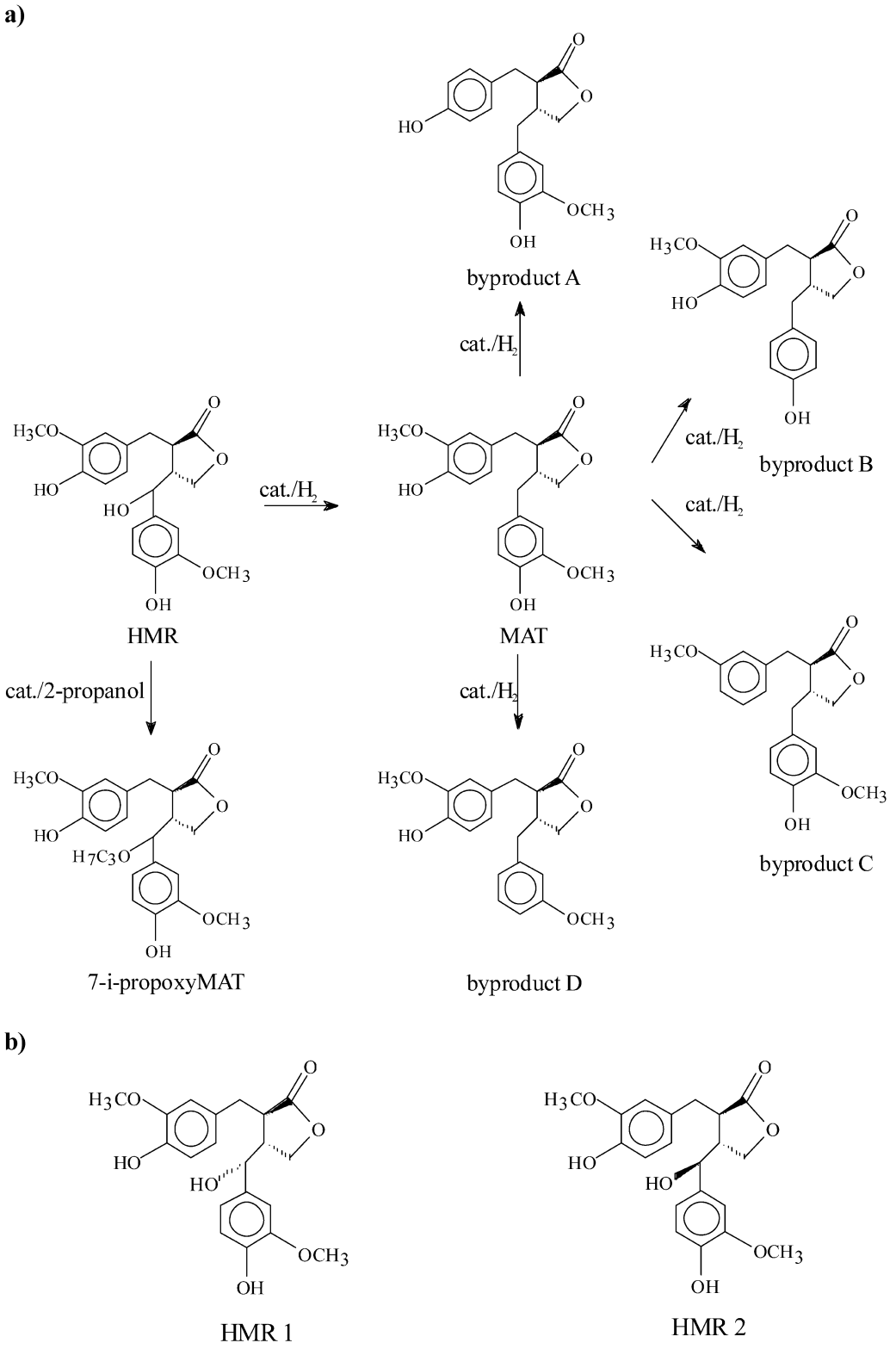

Fig. 1. (a) Reaction scheme, (b) isomers of HMR.

2.3. Experimental procedure

The experiments were performed under atmospheric pressure in a 200-mL glass reactor equipped with a heating jacket (using silicon oil as the heat transfer fluid), a reflux condenser (with the cooling medium set to −20 °C), an oil lock, a pitched-blade turbine, and stirring baffles. In a typical experiment, 100 mg of the catalyst (size of catalyst particles <180 μm) was charged into the reactor. The catalyst was preactivated in situ under hydrogen (AGA, 99.999%) gas flow (100 mL/min) at 100 °C for 1 h (including heating time), after which the reactor was cooled to the reaction temperature of 70 °C under nitrogen

(AGA, 99.999%) gas flow (100 mL/min). When the influence of reduction temperature was studied, the catalyst was reduced at 100 or 200 °C for 1 h ex situ before the in situ activation. The reactant solution, comprising 100 mg of HMR dissolved in 78 g of 2-propanol (J.T. Baker, 99.5%), was deoxygenated under nitrogen gas flow (100 mL/min) for 10 min in a glass tube.

The experiment was started by pouring the reactant solution into the reactor. The reaction time was set to zero, the stirring was started (at 1000 rpm), the gas flow was changed to hydrogen (100 mL/min), and the first sample was withdrawn. The duration of the experiments was 4 h.

Samples were withdrawn at different time intervals and analyzed using a gas chromatograph equipped with a HP-1 column (length 25 m, i.d. 0.20 mm, film thickness 0.11 μm) and a flame ionization detector operating at 300 °C. The samples were silylated before analysis; 100 μL of the sample was dried in a stream of nitrogen gas. To the residue, 80 μL of N,O-bis-(trimethylsilyl)trifluoro-acetamide (BSTFA, 98%, Fluka), 20 μL of trimethylchlorosilane (TMCS, 98%, Acros Organics), and 20 μL of pyridine (99.0%, J.T. Baker) were added. The solutions were kept in an oven at 70 °C for 30 min, then transferred to vials and analyzed by gas chromatography (GC). Then 1 μL of the silylated sample was injected with an autosampler. The injection temperature was 260 °C, and the split ratio was 1:20. Hydrogen served as a carrier gas. The initial temperature of the column was 120 °C (for 1 min), and the temperature was increased at a rate of 6 °C/min to 300 °C (for 10 min). The peaks were identified by analysis with a gas chromatograph–mass spectrometer operating at the same GC conditions.

2.4. Catalyst characterization

The specific surface areas of the supported metal catalysts were measured with a combined physisorption–chemisorption apparatus (Sorptometer 1900, Carlo Erba Instruments). The Dubinin method was used to calculate surface areas of the zeolite-supported palladium catalysts.

The palladium content (wt%) of several zeolites was determined by DCP (ARL SpectraSpan7). Before the analysis, the samples were dried in an oven at 100 °C overnight and stored in an exicator. Then 100 mg of the dried catalyst sample was dissolved in a mixture of 3 mL of hydrofluoric acid and 3 mL of *aqua regia* in a microwave oven. The dissolved sample was diluted with deionized water to 100 mL and analyzed by DCP.

To determine phase purity and structure, the catalyst samples were pretreated at 100 °C in 1 h and stored in acetone, after which they were analyzed by XRPD. The patterns from the analyses were compared with the patterns obtained from pure support materials. The measurements were done on a Bragg–Brentano $\theta/2\theta$ reflection geometry-based Philips PW1820 diffractometer.

To determine the metal particle size and dispersion, samples were analyzed by CO pulse chemisorption (Autochem 2910, Micrometrics). Before the measurements, the samples were dried in an oven at 100 °C overnight and stored in an exicator. Then 100 mg of the sample was placed into a quartz U-tube containing silica wool, the tube was inserted into the system, and the sample was further dried in a stream of helium gas at 50 °C for 30 min. After that, the sample was pretreated at 100 °C for 1 h in hydrogen, using helium as a carrier gas, then flushed with helium (still at 100 °C) for 1 h, cooled to room temperature, and placed in a water bath. Then the CO pulses were introduced (10% CO in helium, helium as a carrier gas) until the adsorption was complete. The dispersion was calculated [17] from the amount of CO consumed, assuming the Pd:CO stoichiometry to be unity [18] and the atomic cross-sectional area to be 0.0787 nm^2.

The acidity of several impregnated zeolites was measured by FTIR (ATI Mattson) using pyridine as a probe molecule for qualitative and quantitative determination of Brønsted acid sites (BAS) and Lewis acid sites (LAS). The pyridine molecule can enter into ring channels of 10 or more members [19]. The catalyst samples were pressed into thin self-supported wafers with a typical weight of 15 mg. The sample was evacuated at 450 °C for 1 h. Pyridine was then adsorbed for 30 min at 100 °C and desorbed by evacuation at different temperatures (250, 350, and 450 °C) to obtain a distribution of acid site strengths. All spectra were recorded at 100 °C. Pyridine adsorbs on BAS and on LAS with corresponding vibration frequencies of 1545 and 1455 cm^{-1}. The concentrations ($\mu mol/g_{cat}$) of BAS and LAS were calculated from the intensities of corresponding bands using the molar extinction coefficients reported by Emeis [20].

3. Results and discussion

3.1. Catalyst properties

Table 1 displays the surface area (Dubinin method), metal content, dispersion, and metal particle size. For the Beta catalysts, the surface area was decreasing in the following order: Pd on H-Beta-300 > H-Beta-150 > H-Beta-25 > H-Beta-11. Pd-H-Beta-300 had the lowest metal content, (only 2 wt%); in the others, metal content varied between 3.9 and 5 wt%. Pd–H-Y had the highest dispersion, followed by Pd–H-Beta-25. Pd on H-Beta-300, H-Beta-150, and H-Beta-11 supports all had approximately the same dispersion. The metal particle size was also obtained from XRPD for palladium on H-Beta-25 and H-Beta-11 (Table 1; values in parentheses). There are problems or limits with both chemisorption and XRPD. For CO chemisorption, one problem is the assumed stoichiometry between metal and CO. The adsorption stoichiometry on large particles (Pd:CO = 2, CO adsorbed in bridged form) is differ-

Table 1
Catalyst properties

Catalyst	Dubinin surface area (m^2/g)	Metal content (wt%)	Dispersion (%)	Metal particle size (nm)[a]
Pd–H-Beta-300	862	2.0	9	13
Pd–H-Beta-150	724	3.9	9	13
Pd–H-Beta-25	691	4.7	13	8 (8)
Pd–H-Beta-11	575	4.1	8	14 (8)
Pd–H-Y	825	5.0	17	7
Pd–H-Mordenite	492	4.6	–	–

[a] Particle size from XRPD in parentheses.

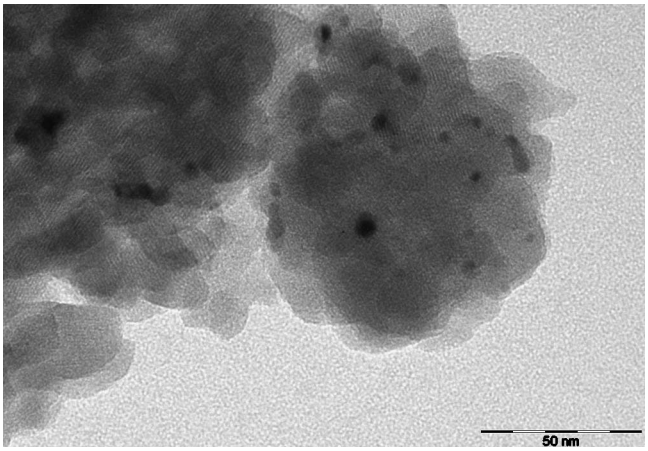

(a)

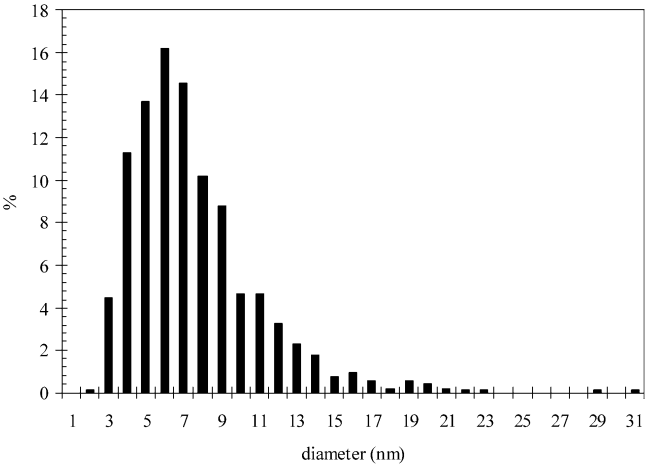

(b)

Fig. 2. Analysis of 2 wt% Pd–H-Beta-300 by transmission electron microscopy: (a) TEM micrograph, (b) size histogram.

ent from that on small particles (Pd:CO = 1, CO adsorbed in linear form), and decreasing particle size results in an increasing fraction of CO adsorbed linearly [18]. This means that if the stoichiometry is assumed to be unity (small particles), but several larger particles are present, then the metal particle size is overestimated. For XRPD, in contrast, the detection limit is around 3 nm, which means that particle size is overestimated here as well. For Pd–H-Beta-25, XRPD gave the same metal particle size as CO chemisorption. For Pd–H-Beta-11, in contrast, the particle size obtained by CO chemisorption was much larger than that obtained by XRPD. This may suggest that the Pd:CO ratio should be greater than unity.

Palladium on H-Beta-300 was also analyzed by TEM. The TEM micrograph and size histogram in Fig. 2 reveal large clusters of particles. The metal particle diameter varied between 2 and 30 nm, and the mean particle size was 7 nm. Thus, it can be concluded that CO chemisorption overestimated the particle size for Pd–H-Beta-300 as well.

Table 2 gives the distribution of acid sites for several palladium-impregnated zeolites. The acidity at 350 and 450 °C for all of the characterized catalysts was negligible, meaning that the palladium-impregnated beta-zeolites contained no strong acid sites. The concentration of weak acid sites (250 °C)

Table 2
Acidity of catalysts

Catalyst	Brønsted acid sites (μmol/g)			Lewis acid sites (μmol/g)		
	250 °C	350 °C	450 °C	250 °C	350 °C	450 °C
2.0% Pd–H-Beta-300	57	0	0	16	0	0
3.9% Pd–H-Beta-150	109	0	0	29	0	0
4.7% Pd–H-Beta-25	161	26	0	75	0	0
4.1% Pd–H-Beta-11	176	20	0	111	8	0
5.0% Pd–H-Y	167	0	0	132	9	3

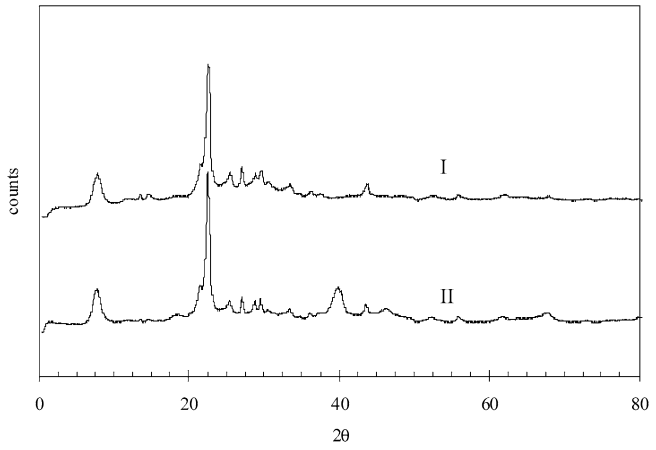

Fig. 3. XRPD pattern of H-Beta (I) and Pd–H-Beta-11 (II).

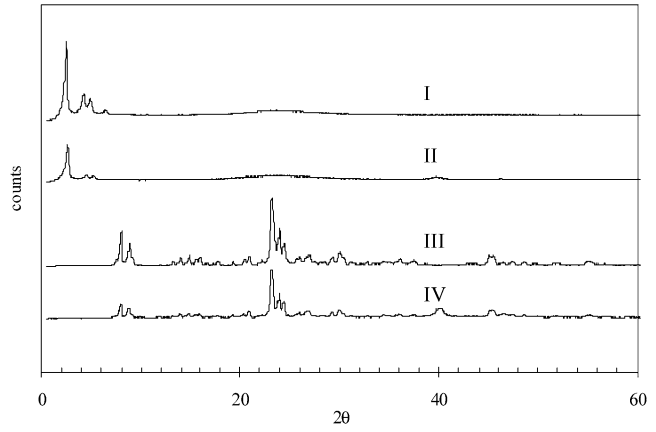

Fig. 4. XRPD pattern of Na-MCM-41 (I), Pd–H-MCM-41 (II), Na-ZSM-5 (III), and Pd–H-ZSM-5 (IV).

follows the Si/Al ratio. Figs. 3 and 4 show the XRPD patterns of the synthesized materials Beta-11, MCM-41, and ZSM-5 both with and without palladium, clearly demonstrating that the impregnation did not affect the structure of the parent materials.

3.2. Activity and selectivity

Fig. 5 reveals that palladium on H-Beta and H-Y gave high reaction rates, and Table 3 demonstrates that the selectivity for all of the catalysts was >90% (at 30 and 60% conversion). Pd–H-Mordenite also worked relatively well (with a conversion of 47% in 4 h), exhibiting the same activity as Pd–H-Beta-11. Palladium on H-MCM-41 and H-ZSM-5 had relatively

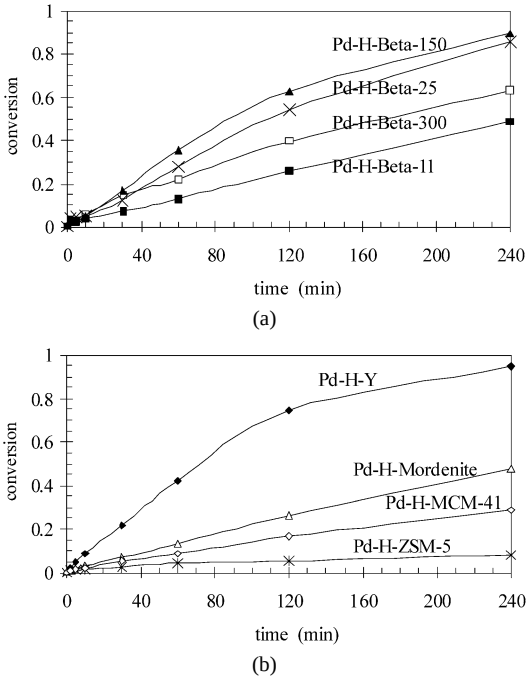

Fig. 5. Hydrogenolysis of HMR over supported palladium catalysts, conversion versus time: (a) ▲, 3.9% Pd–H-Beta-150; ×, 4.7% Pd–H-Beta-25; □, 2.0% Pd–H-Beta-300; ■, 4.1% Pd–H-Beta-11; and (b) ◆, 5.0% Pd–H-Y; △, 4.6% Pd–H-Mordenite; ◇, 5%* Pd–H-MCM-41; and ✳, 5%* Pd–H-ZSM-5. Conditions: 70 °C, 100 mL/min hydrogen gas flow, 2-propanol. *—nominal loading.

Table 3
Selectivity to matairesinol

Catalyst	$Sel_{0.3}$[a]	$Sel_{0.6}$[a]
2.0% Pd–H-Beta-300	0.95	0.94
3.9% Pd–H-Beta-150	0.99	0.97
4.7% Pd–H-Beta-25	0.97	0.96
4.1% Pd–H-Beta-11	0.99	–
5.0% Pd–H-Y	0.95	0.94
5%[b] Pd–H-Mordenite	0.97	–
5%[b] Pd–H-MCM-41	0.99	–

[a] $Sel_{0.3}$ = selectivity to matairesinol at 30% conversion; $Sel_{0.6}$ = selectivity to matairesinol at 60% conversion selectivity = $((c_{MAT}/c_{HMR,tot,0})/\text{conversion})$.
[b] Nominal metal loading.

low conversion: 29 and 8%, respectively, in 4 h. H-Beta-25 without palladium showed no activity, confirming that the reaction requires metal sites. The conversions for Pd/SiO_2 and Pd/Al_2O_3 were only 5 and 9%, respectively, in 4 h. These two catalysts were used as reference samples. One could suppose that because palladium on a less-acidic beta support worked better, alumina or silica would perform better than the zeolites used; however, compared with the tested zeolites, alumina has fewer BAS and more LAS, and silica has even fewer acid sites than alumina [21] (and alumina worked slightly better than silica). Because the activity of Pd/SiO_2 and Pd/Al_2O_3 was low compared with that of Pd/H-Beta, it can be concluded that along with the metal function, Brønsted acidity is also required.

Plotting the initial rates against the density of acid sites for different Beta-zeolites (Fig. 6) clearly shows that a support material with lower acidity gives a higher rate. This superficially

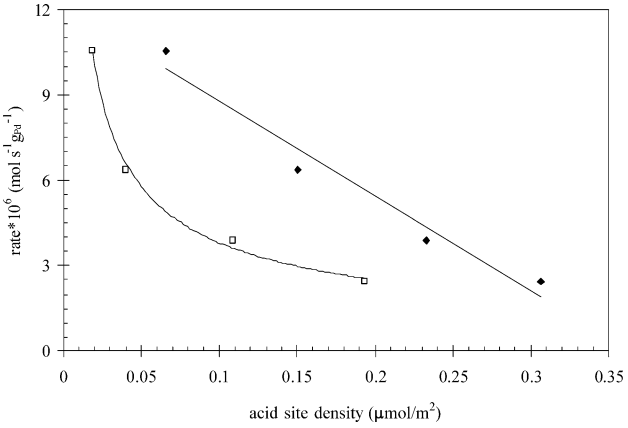

Fig. 6. Initial rate versus acid site density for palladium impregnated Beta-zeolites: ◆, Brønsted acid sites and □, Lewis acid sites. $Rate_{initial}$ = moles of HMR converted after 30 min/(mass of metal × 1800 s). Acid site density = $c_{acid\ sites}$/surface area of support.

contradicts the results obtained with Pd/C [10]. Keep in mind, however, that the intrinsic acidity of carbon-supported materials due to the presence of surface hydroxyl groups is significantly less than that of zeolites. The same relationship with acidity was noted with metal-containing zeolites in hydrogenolysis by Wendlandt et al. [22], who explained the behavior by the metal–support interactions: Acid sites affect the electronic properties of the metal, leading to decreased carbon–metal bonding strength and thus a decreased hydrogenolysis reaction. It has also been stated that metals on acidic supports have higher hydrogenolysis activity compared with metals on neutral or alkaline supports [23]. Several models have been given for the metal–support interactions [23,24]. At present, we can only speculate whether metal–support interactions can explain the dependence on the acidity, especially taking into account rather large size of the palladium particles (Fig. 2; Table 1). Metal–support interactions are operative for small metal particles; particles >1 nm are outside the pores of beta-zeolites, and no interactions between the support and metal can be assumed. Several other explanations (e.g., isomerization from HMR 2 to HMR 1, deactivation, polarity of the support) can be given, and all may be operative to a certain extent.

3.3. Reaction of hydroxymatairesinol

The initial HMR 2/HMR 1 ratio was 3:1. This ratio decreased during the reaction from 3 to approximately 0.6. Fig. 7 shows that the HMR 2/HMR 1 ratio decreased faster in the more acidic supports. In the beginning of the reaction, some isomerization between HMR 2 and HMR 1 (see the chemical formulas in Fig. 1b) was also visible (Fig. 8). Byproducts included 7-isopropoxymatairesinol (7-i-propoxyMAT; two isomers), resulting from interaction with the solvent, as well as four products formed through hydrogenolysis of the functional groups on the benzene rings of MAT (see the reaction scheme in Fig. 1a). Isomerization was greater on the more-acidic catalysts (e.g., Pd–H-Beta-25) than on the less-acidic catalysts (e.g., Pd–H-Beta-300).

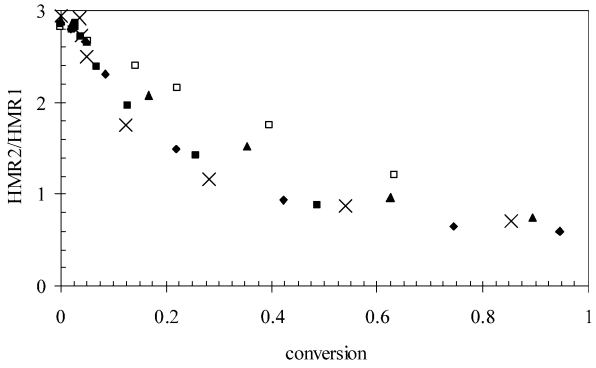

Fig. 7. The HMR 2-to-HMR 1 ratio as a function of conversion. □, 2.0% Pd–H-Beta-300; ▲, 3.9% Pd–H-Beta-150; ×, 4.7% Pd–H-Beta-25; ■, 4.1% Pd–H-Beta-11; and ◆, 5.0% Pd–H-Y.

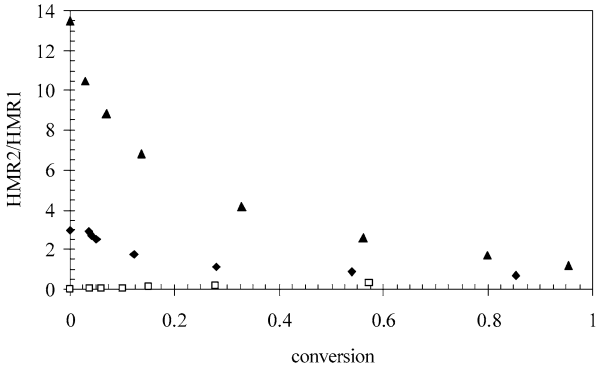

Fig. 10. Hydrogenolysis of HMR over 4.7% Pd–H-Beta-25 at the same conditions as in Fig. 5.

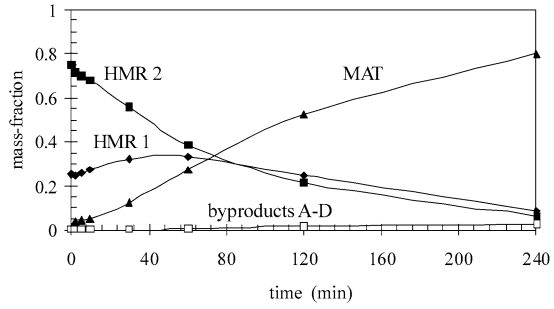

Fig. 8. Hydrogenolysis of HMR over 4.7% Pd–H-Beta-25 at the same conditions as in Fig. 5: ◆, HMR 1; ■, HMR 2; ▲, MAT; and □, byproducts A–D are in Fig. 1. Trace amounts of 7-i-propoxyMAT was also obtained.

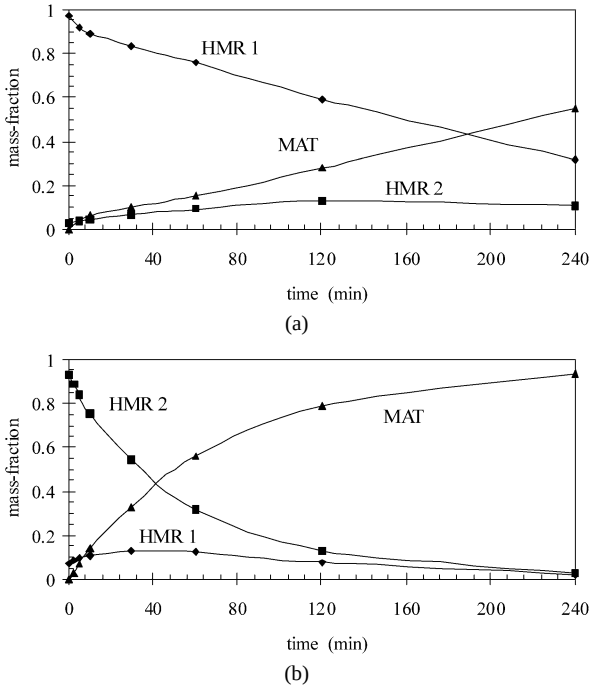

Fig. 9. Hydrogenolysis of HMR over 4.7% Pd–H-Beta-25 at the same conditions as in Fig. 5: ◆, HMR 1; ■, HMR 2; and ▲, MAT are in the figure.

The influence of the ratio between the two isomers was also investigated (Fig. 9). Although the isomers were further separated, totally pure isomers could not be obtained in large quantities. Nevertheless, mixtures containing increased amounts of one isomer and only smaller amounts of the other isomer were prepared. In Fig. 9a, the ratio between HMR 2 and HMR 1 is 0.03 in the beginning; that is, HMR 1 is in great excess. Isomerization of HMR 1 to HMR 2 clearly occurs. In Fig. 9b, the ratio between HMR 2 and HMR 1 is 13.5; HMR 2 is in excess. Here, similar to Fig. 8, isomerization to HMR 1 is clearly visible. A significant difference in the reaction rates between the two isomers is observed. HMR 2 reacts much faster to MAT than HMR 1. Fig. 10 plots the ratio between HMR 2 and HMR 1 as a function of the conversion for three different starting ratios: HMR 2/HMR 1 = 13.5 (HMR 2 in excess), 3 (ratio corresponding to extractives from wood knots), and 0.03 (HMR 1 in excess). The HMR 2/HMR 1 ratio decreases from 13.5 to 1.2 in the first mixture, decreases from 3 to 0.7 in the second mixture, and increases from 0.03 to 0.34 in the third mixture. The fact that HMR 2 reacts much faster to MAT than HMR 1 and that isomerization of HMR 2 to HMR 1 increases with a more-acidic zeolite could explain in part why a less-acidic zeolite is preferred; the hydrogenolysis reaction is retarded by the isomerization of the faster-reacting isomer to the slower-reacting isomer.

An experiment under nitrogen atmosphere was performed for the isomer mixture with an HMR 2/HMR 1 ratio of 13.5 to evaluate the effect of atmosphere on the reaction (Fig. 11a). The catalyst was preactivated as before with hydrogen at 100 °C. The major product was oxomatairesinol (oxoMAT; Fig. 11b), but smaller amounts of MAT and 7-i-propoxyMAT were also obtained. The oxoMAT is most probably a result of HMR dehydrogenation, catalyzed by palladium. It follows from Fig. 11a that HMR 2 isomerizes to HMR 1 also under nitrogen atmosphere. It cannot be unequivocally concluded whether or not this isomerization requires hydrogen, because hydrogen is available on the surface due to pretreatment and/or dehydrogenation.

3.4. Reduction temperature

The catalysts were preactivated in situ at 100 °C for 1 h under hydrogen flow in the experiments described above. The influence of the reduction temperature was also investigated for the catalyst that gave the highest TOF, Pd–H-Beta-300. The

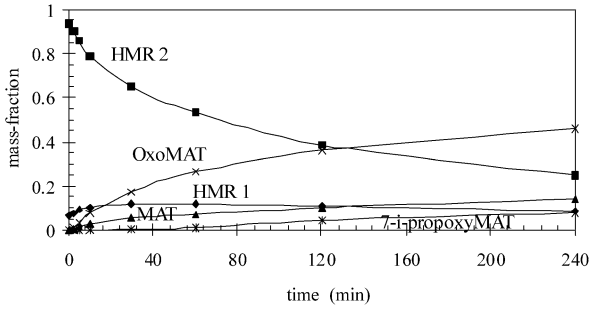

(a)

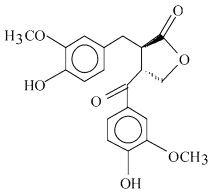

(b)

Fig. 11. (a) Hydrogenolysis of HMR over 4.7% Pd–H-Beta-25: ◆, HMR 1; ■, HMR 2; ▲, MAT; ×, oxoMAT; and ⚹, 7-i-propoxyMAT are in the figure. (b) Structure for oxomatairesinol (oxoMAT). Conditions: 70 °C, 100 mL/min nitrogen gas flow, 2-propanol.

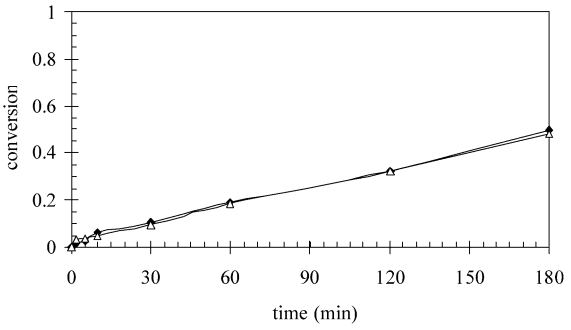

Fig. 12. Hydrogenolysis of HMR over 2.0% Pd–H-Beta-300 pre-treated ex situ under hydrogen flow at different temperatures: ◆, 100 °C and △, 200 °C. Activation in situ at 100 °C under hydrogen flow was done prior to the experiments. Experimental conditions: 70 °C, 100 mL/min hydrogen gas flow, 2-propanol.

catalyst was first treated ex situ under hydrogen flow at either 100 or 200 °C for 1 h, followed by the same preactivation as in the catalyst screening experiments done in situ. Fig. 12 shows that the catalysts pretreated at different temperatures gave the same activity, indicating that reduction at 100 °C is sufficient to achieve an active catalyst.

4. Conclusion

Hydrogenolysis of hydroxymatairesinol to matairesinol was performed over palladium-supported catalysts under hydrogen and nitrogen atmospheres. A variety of supports, including zeolites with varying structures and acidities, were tested. Results for palladium on H-Beta with varying acidities demonstrated that the reaction rate is inversely proportional to the acidity. However, Brønsted acidity is needed, because palladium on SiO_2 and Al_2O_3 was not active. In addition to the acidity, metal is needed; H-Beta-25 support without palladium displayed no activity. Evaluation of the effect of the initial ratio between the isomers revealed that isomerization from the major isomer to the minor isomer occurs. Moreover, the HMR 2 isomer reacts faster in hydrogenolysis than the HMR 1 isomer. When the reaction was conducted under nitrogen atmosphere, the major product was oxomatairesinol.

Acknowledgments

This work is part of the activity at the Åbo Akademi Process Chemistry Centre within the Finnish Centre of Excellence Programme (2000–2005) by the Academy of Finland. Financial support from the Raisio Group Research Foundation and European Union through the Sixth Framework Programme is gratefully acknowledged. The authors thank Christer Eckerman for the HMR preparation, Markku Reunanen for the GC-MS analysis, and Drs. Stan Dzwigaj and Eric Marceau for the TEM analysis.

References

[1] H. Adlercreutz, Lancet 3 (2002) 364.
[2] S.M. Willför, M.O. Ahotupa, J.E. Hemming, M.H.T. Reunanen, P.C. Eklund, R.E. Sjöholm, C.S.E. Eckerman, S.P. Pohjamo, B.R. Holmbom, J. Agric. Food Chem. 51 (2003) 7600.
[3] D.C. Ayres, J.D. Loike, Lignans—Chemical, Biological and Clinical Properties, Cambridge Univ. Press, Cambridge, 1990, p. 1.
[4] N.M. Saarinen, A. Wärri, S.I. Mäkelä, C. Eckerman, M. Reunanen, M. Ahotupa, S.M. Salmi, A.A. Franke, L. Kangas, R. Santti, Nutr. Cancer 36 (2000) 207.
[5] S. Willför, J. Hemming, M. Reunanen, C. Eckerman, B. Holmbom, Holzforschung 57 (2003) 27.
[6] P. Eklund, R. Sillanpää, R. Sjöholm, J. Chem. Soc., Perkin Trans. 1 (2002) 1906.
[7] S. Heinonen, T. Nurmi, K. Liukkonen, K. Poutanen, K. Wähälä, T. Deyama, S. Nishibe, H. Adlercreutz, J. Agric. Food Chem. 49 (2001) 3178.
[8] G.V. Smith, F. Notheisz, Heterogeneous Catalysis in Organic Chemistry, Academic Press, San Diego, 1999, p. 131.
[9] S. Nishimura, Handbook of Heterogeneous Catalytic Hydrogenation for Organic Synthesis, Wiley, New York, 2001, p. 447.
[10] H. Markus, P. Mäki-Arvela, N. Kumar, N.V. Kul'kova, P. Eklund, R. Sjöholm, B. Holmbom, T. Salmi, D.Yu. Murzin, Catal. Lett. 103 (2005) 125.
[11] N. Krishnankutty, M.A. Vannice, J. Catal. 155 (1995) 312.
[12] W.F. Hölderich, H. van Bekkum, Stud. Surf. Sci. Catal. 137 (2001) 821.
[13] A. Corma, G. Hermeneglido, Catal. Today 38 (1997) 257.
[14] R.L. Wadlinger, G.T. Kerr, E.J. Rosinski, US Patent 3 308 069 (1975), to Mobil Oil Corporation.
[15] T.A.J. Hardenberg, L. Mertens, P. Mesman, H.C. Muller, C.P. Nicolaides, Zeolites 12 (1992) 685.
[16] C.T. Kresge, M.E. Leonowicz, W.J. Roth, J.C. Vartuli, US Patent 5 098 684 (1992), to Mobil Oil Corporation.
[17] G. Bergeret, P. Gallezot, in: G. Ertl, H. Knözinger, J. Weitkamp (Eds.), Handbook of Heterogeneous Catalysis, vol. 2, Verlagsgesellschaft mbH, Weinheim, 1997, p. 439.
[18] T.A. Dorling, R.L. Moss, J. Catal. 7 (1967) 378.
[19] A. Jentys, J.A. Lercher, Stud. Surf. Sci. Catal. 137 (2001) 345.
[20] C.A. Emeis, J. Catal. 141 (1993) 347.
[21] P. Mäki-Arvela, N. Kumar, V. Nieminen, R. Sjöholm, T. Salmi, D.Yu. Murzin, J. Catal. (2004) 155.
[22] K.-P. Wendlandt, H. Bremer, F. Vogt, W.P. Reschetilowski, W. Mörke, H. Hobert, M. Weber, K. Becker, Appl. Catal. 31 (1987) 65.
[23] B.L. Mojet, J.T. Miller, D.E. Ramaker, D.C. Koningsberger, J. Catal. 186 (1999) 373.
[24] D.C. Koningsberger, J. de Graaf, B.L. Mojet, D.E. Ramaker, J.T. Miller, Appl. Catal. A 191 (2000) 205.